

## Supplementary material

### **The role of charge on the diffusion of solutes and nanoparticles (silicon nanocrystals, nTiO<sub>2</sub>, nAu) in a biofilm**

*Mahmood Golmohamadi,<sup>A</sup> Rhett J. Clark,<sup>B</sup> Jonathan G. C. Veinot<sup>B</sup> and Kevin J. Wilkinson<sup>A,C</sup>*

<sup>A</sup>Department of Chemistry, University of Montreal, PO Box 6128, Succursale Centre-ville, Montréal, QC, H3C 3J7, Canada.

<sup>B</sup>Department of Chemistry, University of Alberta, 11227 Saskatchewan Drive, Edmonton, AB, T6G 2G2, Canada.

<sup>C</sup>Corresponding author. Email: [kj.wilkinson@umontreal.ca](mailto:kj.wilkinson@umontreal.ca)

### **The structures and optical information on the fluorescent probes**

In order to investigate the effect of charge in the biofilms, several variably charged fluorescent solutes were employed. The structures of probes along with their fluorescence spectra are given in Table S1.

**Table S1. The structure and fluorescence spectra of small fluorescent probes**

z, charge of the fluorescent probes

Probe	Structure	z	$d_H$ (nm)	Absorption and emission spectra
Tetramethylrhodamine, methyl ester (TMRM) <sup>A</sup>		+1	1.24	
Rhodamine B (RB) <sup>B</sup>		0	1.14	
Oregon green 488 carboxylic acid, succinimidyl ester (Oregon Green 1C) <sup>A</sup>		-1	1.22	
Oregon green 488 carboxylic acid (Oregon Green 2C) <sup>A</sup>		-2	1.32	

<sup>A</sup>Spectra were taken from [www.invitrogen.com](http://www.invitrogen.com).

<sup>B</sup>Spectra taken from [www.iss.com](http://www.iss.com).

### **Preparation of the silicon nanocrystals**

The complete synthesis of the silicon nanocrystals can be found in Clark et al.<sup>[1]</sup> Briefly, Si-NC were produced in a silica matrix composite by high temperature processing of hydrogen silsesquioxane in methyl isobutyl ketone (HSQ purchased from Dow Corning under the tradename FOx-16) under a slightly reducing atmosphere. In total 1 g of silicon composite was etched with hydrofluoric acid in the presence of ethanol and water in order to liberate the particles from the silica matrix. The particles were then extracted from the water with three portions of toluene and transferred to a flame-dried custom Schlenk flask that was equipped with a quartz sleeve. Methyl undecanoate (0, 10, 25, 50, 100 or 200  $\mu\text{L}$ ) was added to the flask. Oxygen was removed from the reaction mixture by applying three freeze–pump–thaw cycles. The reaction was initiated by inserting two UV LEDs (Nichia America Corp., 250 mW at 365 nm, 3.4 eV) into the quartz sleeve and irradiating the mixture for 2 h. A total of 4 mL of undecylenic acid was then added and the reaction was left to react for another 15 h. Upon completion of the reaction, the clear, colourless supernatant was decanted and the functionalised particles, which were present as a precipitate, were dispersed in ethanol. The suspension was transferred into test-tubes with an excess of toluene, before centrifuging at 1520g (The Drucker Co., Laboratory Centrifuge, model 614) for 15 min at 23 °C. The supernatant was again removed and the solid redispersed in ethanol. This procedure was repeated once more with toluene and once with pentane. Finally, the remaining particles were dispersed in ethanol for storage and characterisation. Water suspensions of the surface functionalised Si-NCs were obtained by slowly diluting the Si-NCs with a mixture containing 5 mL of ethanol per 5 mL of water. The majority of the ethanol was removed by rotoevaporation and the remaining solution was transferred to dialysis tubes (8–10 kD cellulose ester). Dialysis was carried out in distilled water with the water being changed at least two additional times with a minimum of 3 h between changes.

### **FCS of the probes and nanoparticles in water and biofilm**

The correlations of the fluorophore Org 2C and the  $n\text{Si}_1$  in water and in the biofilm are shown in Fig. S2. For both the diffusion of Org 2C (Fig. S2a) and the  $n\text{Si}_1$  nanoparticles (Fig. S2b), the autocorrelation function was shifted to longer diffusion times when measurements were made in the biofilm. Furthermore, the greater the density of the biofilm, the greater was the displacement towards longer diffusion times (zones 1, 2, 3 in Fig. S2b). Finally, careful comparison of the curves obtained in water for the Org 2C (Fig. S2a) with respect to the  $n\text{Si}_1$  (Fig. S2b) show that the larger particle diffused more slowly.

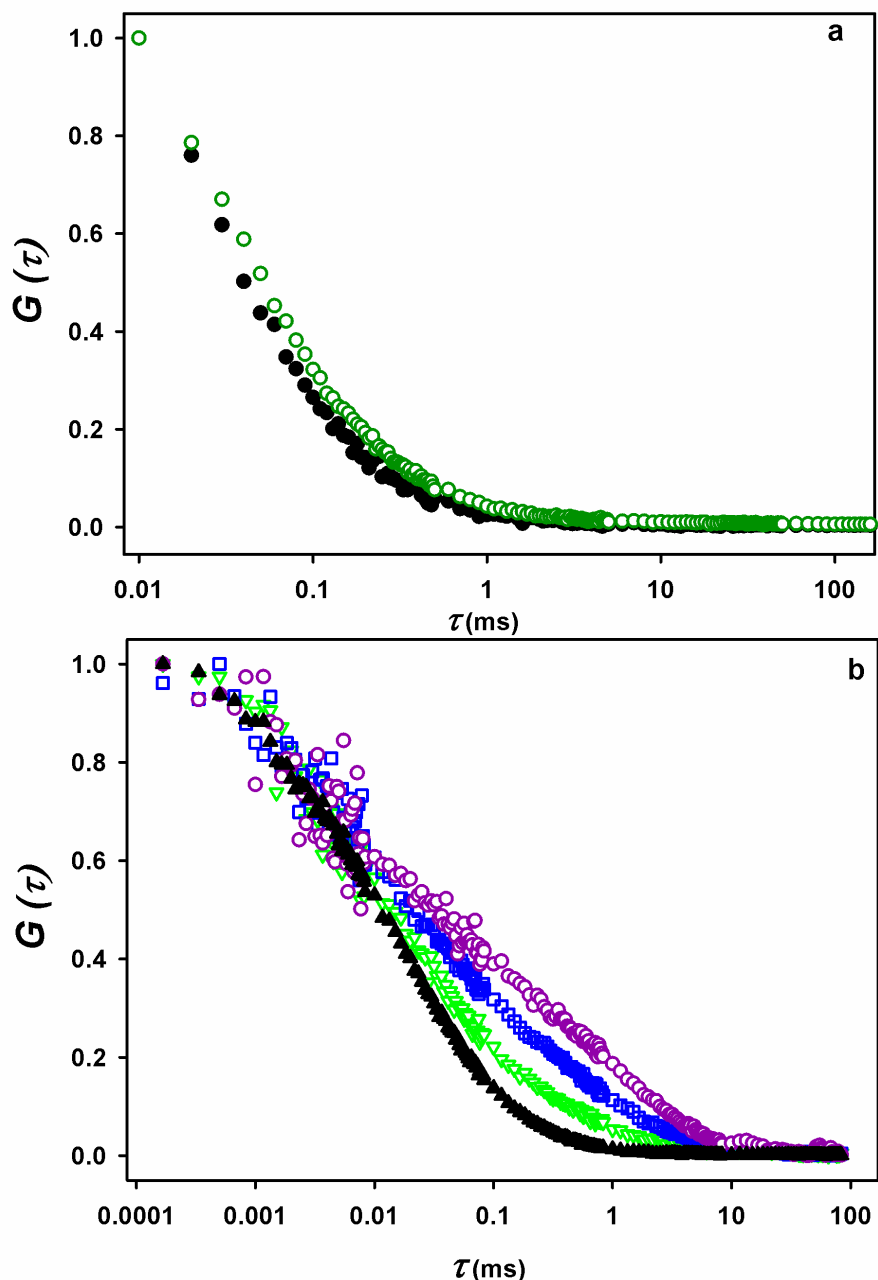


**Fig. S1.** (a) The fluorescence correlation of Oregon 2C in water (●) superimposed on that of biofilm (○);  $c = 20$  nM; pH = 7.1;  $I = 1$  mM; laser: 488 nm; laser intensity:  $40 \mu\text{W}$ ; acquisition time = 60 s; acquisition frequency =  $10^5$  Hz (resolution time: 10  $\mu\text{s}$ ). (b) The fluorescence correlation of  $nSi_1$  in water (▲) superimposed on that of variably dense zones of biofilm: less dense part of EPS matrix (▽), an intermediate density (□) and the most dense part of the biofilm (○);  $c_{nSi} = 30$  mg  $\text{L}^{-1}$ ; pH = 7.1;  $I = 1$  mM; laser intensity:  $40 \mu\text{W}$ ; acquisition time = 60 s; acquisition frequency =  $10^7$  Hz (resolution time: 0.1  $\mu\text{s}$ ).

### Background fluorescence of the biofilm

For several samples, a background signal appearing in the FCS correlations of the biofilms was observed. It was attributed to either the sorption of fluorescent nanoparticles to the biofilm matrix or to the autofluorescence of the biofilm. Indeed, the auto-fluorescence of the biofilm is known to result in large part from the water soluble pyoverdines that are produced by the bacteria and associated with the PS matrix.<sup>[2,3]</sup> Nonetheless, because FCS is based on the analysis of fluorescence intensity fluctuations, constant background fluorescence does not generally influence the measured diffusion times. In contrast, the overall movement of (a fluorescent) biofilm can lead to fluctuations of the fluorescence signal; however, they are generally at much longer correlation times. For example, translational diffusion times of  $\tau_D > 0.5$  s were attributed to the background movement of the biofilm, much greater than the corresponding diffusion times that were obtained for the fluorescent probes ( $\tau_D < 30$   $\mu$ s) and nanoparticles ( $\tau_D < 2$  ms). Although the background fluorescence makes quantification of the fluorescence fluctuation signal more difficult (e.g. blue line, Fig. S2), the background signal can be corrected through the introduction of a constant parameter  $b$  in the Gaussian model (e.g. dashed red line, Fig. S2). The small modelled value for  $b$  can lead to very significant differences in the diffusion coefficient for the nanoparticles (Table S2).

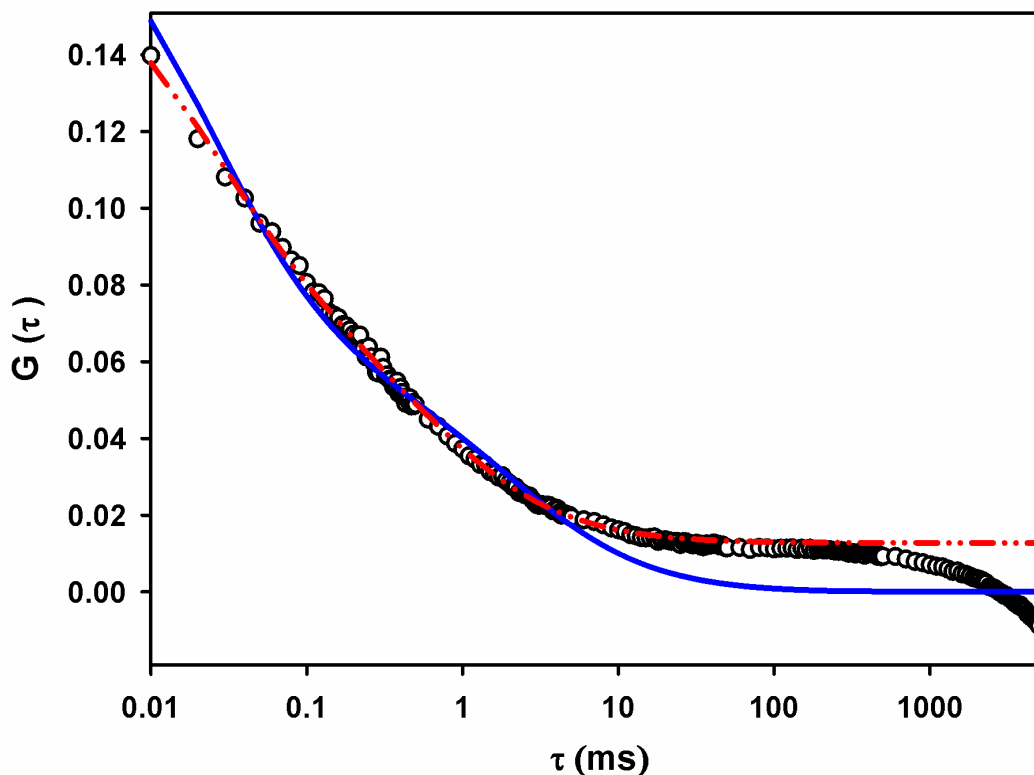


**Fig. S2.** FCS correlation curves for the diffusion of the nSi<sub>6</sub> nanoparticle. Black circles are experimental data obtained with a significant background signal. The solid blue line is the fitted line obtained without taking into account the constant displacement, whereas the dashed red line takes into account the background fluorescence through the use of the parameter *b* (Eqn 1); *c* = 30 mg L<sup>-1</sup>; pH = 7.1; *I* = 1 mM; laser: 488 nm; laser intensity: 40 μW; acquisition time = 60 s; acquisition frequency = 10<sup>5</sup> Hz, resolution time = 10 μs.

**Table S2. Diffusion coefficients of nanoparticle of nSi<sub>6</sub> in biofilm with and without correction of background signal**

	$D_{R123}$ (10 <sup>-10</sup> m <sup>2</sup> s <sup>-1</sup> )	$D_{nSi6}$ (10 <sup>-10</sup> m <sup>2</sup> s <sup>-1</sup> )	$\omega_{xy}$ (μm)	$\omega_z$ (μm)	<i>b</i>	$\chi^2$
Solid blue line	440	4.6	0.21	1.35	–	5.1
Dashed red Line	440	15.5	0.21	1.35	0.0128	0.34

### Labelling the gold and titanium nanoparticles with oppositely charged probes

When the labelling of the nAu and nTiO<sub>2</sub> nanoparticles was performed with fluorescent probes of opposite charge (R123 and Org 1C), diffusion coefficients were reduced significantly with respect to the results obtained with similarly charged probes (Fig. 4). Nonetheless, despite of the agglomeration of the probes in water, similar conclusions could be drawn as for the non-aggregated probes (Fig. S3), i.e. diffusion was slowed for the nAu more than for the nTiO<sub>2</sub>, since the  $D_b/D_w$  values were very similar to those found with non-aggregated probes.

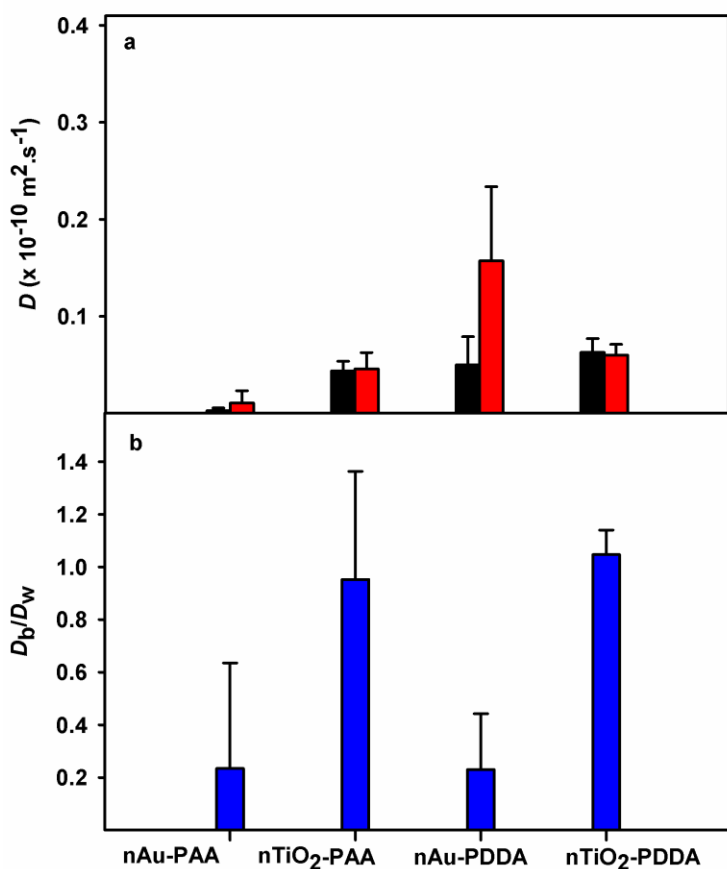


**Fig. S3.** Diffusion coefficients obtained when the nanoparticles were labelled with oppositely charged fluorescent probes: (a) diffusion coefficient of nAu and nTiO<sub>2</sub> in the biofilm,  $D_b$  (black columns) and in water,  $D_w$  (red columns). NPs were labelled with rhodamine 123 and Oregon 1C; (b) the ratio of  $D_b/D_w$  (blue columns) for nAu and nTiO<sub>2</sub>. NPs were labelled with R123 and Org 1C;  $c = 30 \text{ mg L}^{-1}$ ;  $I = 1 \text{ mM}$  (MOPS);  $\text{pH} = 7.1$ . Error bars correspond to the standard deviations of  $n = 15\text{--}20$  for FCS measurements.

### Agglomeration of nanoparticles

Agglomeration of the nanoparticles was sometimes observed in solutions that were left to age or under specific physicochemical conditions. Agglomeration could be detected by following the NP with time or by cross correlating the two FCS channels (two colours) (Fig. S4).

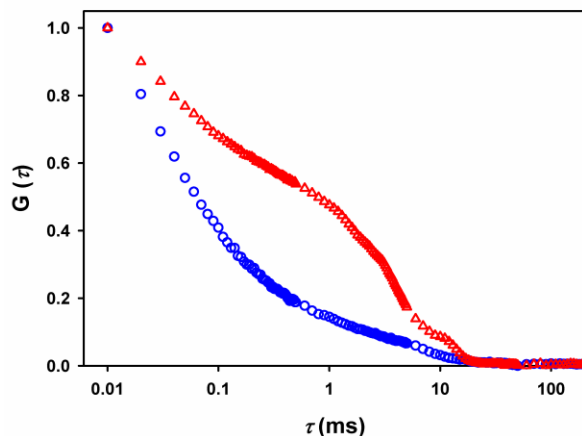


**Fig. S4.** FCS cross-correlation curves for the  $n\text{Si}_2$  nanoparticles in water ( $\text{pH} = 7.1$ ,  $I = 1 \text{ mM}$ ) as shown by the blue circles in cross-correlation curves due to the agglomeration of nanoparticle of  $n\text{Si}_2$  in water were detected for nanoparticles that were aged 3 weeks ( $\Delta$ ).

### Nature of the biofilm and biofilm measurements

The *Pseudomonas* biofilm has been characterised previously in our laboratory using confocal laser microscopy (Fig. S5)<sup>[3]</sup>:

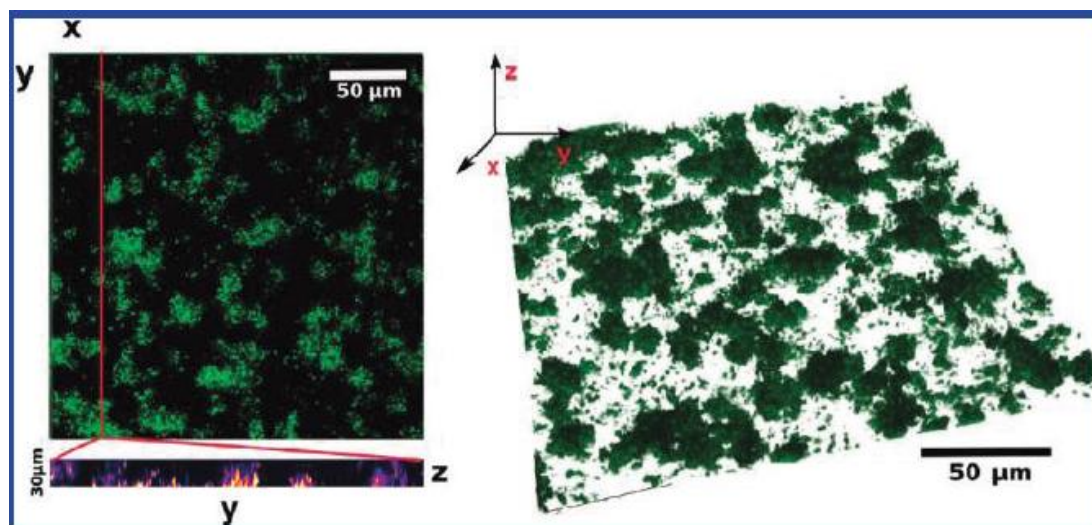


**Fig. S5.** CSLM images of the *Pseudomonas fluorescens* biofilm.<sup>[3]</sup>



The average thickness of biofilm was  $\sim 10\text{--}30\ \mu\text{m}$  (Fig. S6). Diffusion measurements in the biofilm were performed at a distance of  $10\ \mu\text{m}$  from the coverslip whereas ‘bulk solution’ measurements were performed  $100\ \mu\text{m}$  above the coverslip (Fig. S6).

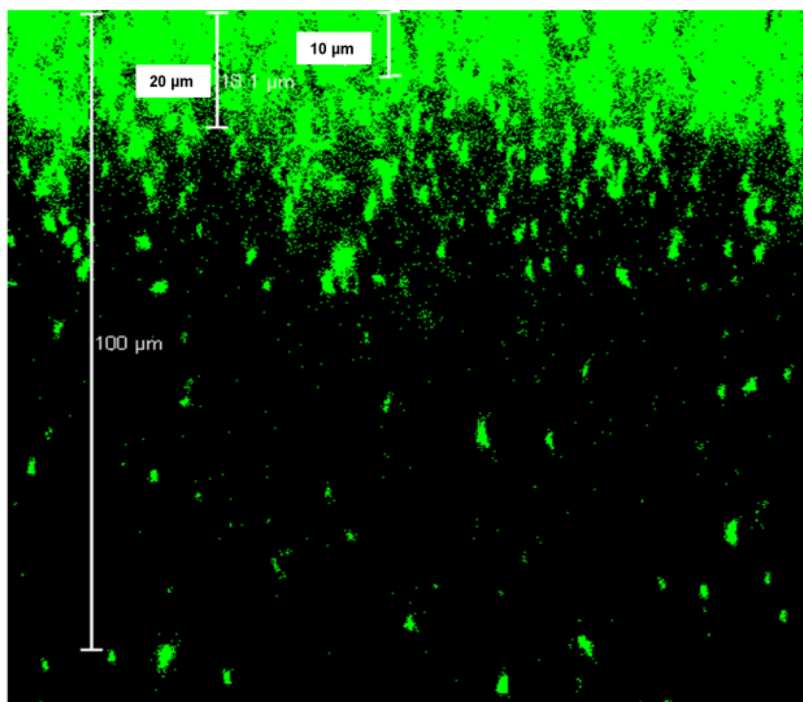


**Fig. S6.** CSLM imaging of the *Pseudomonas fluorescens* biofilm in the XZ direction.

The main reason that numerous spots in biofilm were scanned (15–25 replicates) was in order to average out effects due to biofilm heterogeneity. Much of the complexity is due to the nature of the EPS and the accompanying water channels in the cell clusters.

## References

- [1] R. J. Clark, M. K. M. Dang, J. G. C. Veinot, Exploration of organic acid chain length on water-soluble silicon quantum dot surfaces. *Langmuir* **2010**, *26*, 15657. doi:10.1021/la102983c
- [2] R. P. Elliott, Some properties of pyoverdine, the water-soluble fluorescent pigment of the pseudomonads. *Appl. Microbiol.* **1958**, *6*, 241.
- [3] T. O. Peulen, K. J. Wilkinson, Diffusion of nanoparticles in a biofilm. *Environ. Sci. Technol.* **2011**, *45*, 3367. doi:10.1021/es103450g